Materials Research. 2020; 23(5): e20200283
DOI: https://doi.org/10.1590/1980-5373-MR-2020-0283

Recrystallization Study of the Al4.5wt%Cu Alloy Conventionally and Unidirectionally Solidified, Deformed and Heat Treated

Roberta Alves Gomes Matos[a]*, *Jonas Mendes*[a], *Bruna Horta Bastos Kuffner*[a], *Mirian de Lourdes Noronha Motta Melo*[a], *Gilbert Silva*[a]

[a]*Universidade Federal de Itajubá (UNIFEI), Itajubá, MG, Brasil*

Received: June 26, 2020; Revised: August 17, 2020; Accepted: September 26, 2020

The Al4.5wt%Cu is an aeronautical and automobile alloy with extensive use in industry for structural purposes. The aim of this work was to evaluate two different solidification processes of the Al4.5wt%Cu alloy, conventional and unidirectional, as well as its recrystallization process. Firstly, the Al4.5wt%Cu alloy was deformed by cold rotary forging and then heat treated at temperatures that varied from 250 to 450 °C. The samples for analysis were obtained after 54, 76 and 91% of reductions in area. Tests of optical microscopy, scanning electron microscopy and Vickers microhardness were performed to evaluate the recrystallization process. The results indicated that the recrystallization started at 350 ºC, being that the conventional samples presented full recrystallization after 5 minutes, while the unidirectional samples presented only partial recrystallization. In general, both solidification processes presented similar results for all of the analysis performed.

Keywords: *Al4.5wt%Cu alloy; Conventional and Unidirectional Solidification; Rotary Swaging Process; Recrystallization Temperature; Recrystallization Kinetics.*

1. Introduction

Aluminum alloys (AA) are widely used in aeronautical and automobile industries. Some characteristics of these alloys incluse low density, good corrosion resistance, high strength, good thermal and electric conductivity. They are considered the most used metallic materials, after iron and steel. According to microstructure and chemical compositions, they can be classified as cast (content of alloying elements between 10 to 12%) or wrought (content of alloying elements between 1 to 2%). Also, these alloys can be divided in two types: heat treatable and non-heat treatable. This definition is directly related to the response of the alloy to precipitation hardening. The heat treatments most commonly applied in AA include annealing, quenching, precipitation hardening, homogenization and aging at elevated or room temperatures[1-5].

The Al-Cu alloys are highly applied among the AA. After casting, they acquire heterogeneous microstructures, and what differentiates each one is the copper content in its chemical composition. The most used Al-Cu alloys are those containing between 4 and 10% in weight of Cu. The main advantage that the copper provides is related to the mechanical properties, such as increase in fatigue strength and hardness. The Al4.5wt%Cu belongs to the family of Al-Cu alloys, and calls attention due to its great potential to be heat treated. A very usual precipitate or intermetallic formed in this family is the $CuAl_2$. This phase has the ability to provide a primary strengthening to the ductile AA matrix[6-10].

In metallurgy, the grain structure of casted materials is considered a very important parameter to understand. The microstructure that the material will present after cooling is directly associated with the solidification method applied. Also, subsequent processes like cold working, which leads the material to plastic deformations, and the application of heat treatments, have the capacity to change this microstructure. The combination of all of these factors defines the final mechanical properties of the material[11,12].

Usually, two microstructures can be obtained after the solidification processes of aluminum alloys, which are equiaxed or columnar dendrites. Dendritic microstructures are formed in casted and welded alloys. Knowing that one determinant factor in metal properties is the dendritic growth, its direction is considered very important in the microsegregation and distribution of secondary phases. In face centered cubic alloys, normally trunks of primary dendrite grow along typical {100} direction, and the dendrite tips are bounded by slowest growing closed-packed {111} planes[13,14].

Equiaxed and columnar dendrites are considered very common morphologies found in casted metallic materials. The growth of equiaxed dendrites happen by the formation of small nuclei, inside of a supercooled melt or attached to the wall of a mold. The nuclei in free condition develop instabilities very quickly at the interface solid/liquid, growing then in the form of equiaxed dendrites. Already columnar dendrites are formed in directional casting processes. During solidification, nucleated seeds with random orientations are formed in the surface of the chill casted material. After this, these seeds grow along preferred crystalline orientations as columnar dendrites. During solidification, the grains with {100} crystallographic orientations best aligned with the vertical heat flow direction grow preferentially at the expense of grains with less favorably orientation. It happens due to

*e-mail: ro.alves@ymail.com

the {100} priority growth of dendrites, componentes of the grains. Thus, as the columnar grains grow directionally, their density in a transverse section decreases. This mechanism of grain selection is currently used in industry to produce single-crystal turbine blades. Dendritic growth is one of the most difficult solidification patterns to obtain. Also, the most prevalent form of crystallization in technology and nature[15-19].

The recrystallization of metals and alloys that were previously plastically deformed is very important, due to two main reasons: Restore and soften the ductility of the material hardened by low temperature deformation, which happens below 50% of the melting temperature, and to control the grain structure of the final material. In metals, the structure of the grain is modified by phase transformation. In the case of other metallic alloys, especially those based on copper, nickel, and aluminum, the recrystallization after deformation is the only method to produce a new grain structure. It happens through the modification of its shape, size, texture and orientation. The driving force used in recrystallization is the stored energy accumulated in the microstructure of the material during plastic deformation (PD). The greater is the PD, the lower will be the temperature needed to recrystallize the material. Also, higher will be the presence of new grains, due to more nucleation sites. This PD is obtained from cold-working processes[20-25].

A widespread method of grain refinement is based on PD at room temperature, followed by elevated annealing temperature. Other method is the production of new grains during hot working, through dynamic recrystallization. For both one and the other, the resultant microstructure is from the production of recrystallization nuclei and long-range migration of the grain boundaries. The processes quoted occur in two steps, being then considered discontinuous. Another approach for new grains formation happens under conditions of severe PD. In this, ultrafine grained structures are developed at low temperatures[26,27].

Although the Al4.5wt%Cu alloy is one of the most used alloys in aeronautical and automotive industries, it is usually produced from conventional casting method. Thus, this research aimed to investigate the microstructural differences between the Al4.5wt%Cu alloy alloy produced through conventional solidification, which gives rise to equiaxed dendritic grains, and the same alloy produced through unidirectional solidification, which originates columnar dendritic grains. Also, PD using rotary swaging was performed in the two materials, in order to determine the best recrystallization temperature for both conditions. It is considered very important to find the lowest possible energy to be inserted into the process.

2. Experimental

In this work, the Al4.5wt%Cu alloy was submitted to two different types of solidification (conventional and unidirectional), in order to define the best condition. For the conventional solidification process, a bar of Al4.5wt%Cu alloy was obtained directly from the traditional casting process, being then machined until achieve dimensions of 15 mm of diameter and 135 mm of length. This machining was performed to unify the two bars of each condition to the same dimensions. For the unidirectional solidification process, 32 grams of Al4.5wt%Cu alloy were casted in a Brasimet® electric furnace, at temperature of 750 ºC during 60 minutes. Air atmosphere was used, once that aluminum alloys do not suffer oxidation at high temperatures. After casting, the alloy was introduced into a mold of 18 mm of diameter and 135 mm of length, being then demolded and machined to a diameter of 15 mm.

The longitudinal section of both solidification processes was chosen for analysis, once that it shows in more detail their microstructures. Figure 1 shows a sample divided in two parts, that corresponds to the same macrostructures obtained in this research, according to[28]. After conventional solidification (Figure 1a), the grains presented equiaxed dendritic structure. Already for the unidirectional solidification, columnar dendritic grains were formed. The main difference observed between both solidification processes is the morphology of the grains. In conventional solidification, the grains presented rounded morphology, while for unidirectional solidification, the grains presented elongated morphology. In the two morphologies, it is possible to observe the dendrites. However, in the unidirectional solidification process, it is more evident the elongated grains then the dendrites.

After the obtainment, both bars were cold rotary forged by rotary swaging method. In each RA, a sample was removed, totalizing 3 samples for each condition. Table 1 shows the parameters used in the swaging process. The RA per pass were limited according to the design of the dies inlet cone, as well as the reduction capacity of the rotary swaging machine. The tensile strength, hardness and RA of each pass are the parameters that affect the material forging. Also, the microstructural characteristics influence directly the ease of forging[29].

After this process, each type of RA was sectioned in 5 samples, to be isothermally treated by annealing at

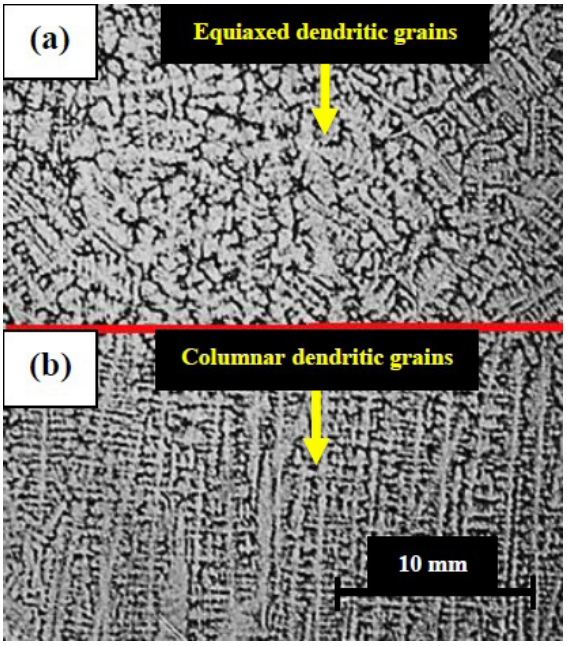

Figure 1. Example of macrostructures of (a) Equiaxed dendritic grains (b) Columnar dendritic grains[28].

Table 1. Parameters used in the rotary swaging process.

Sample	Point reduction in area (%)	Initial Diameter (mm)	Final Diameter (mm)	Reduction in diameter (%)
1	54	9.525	10.2	16.34
2	76	6.350	7.4	20
3	91	4.369	4.7	18

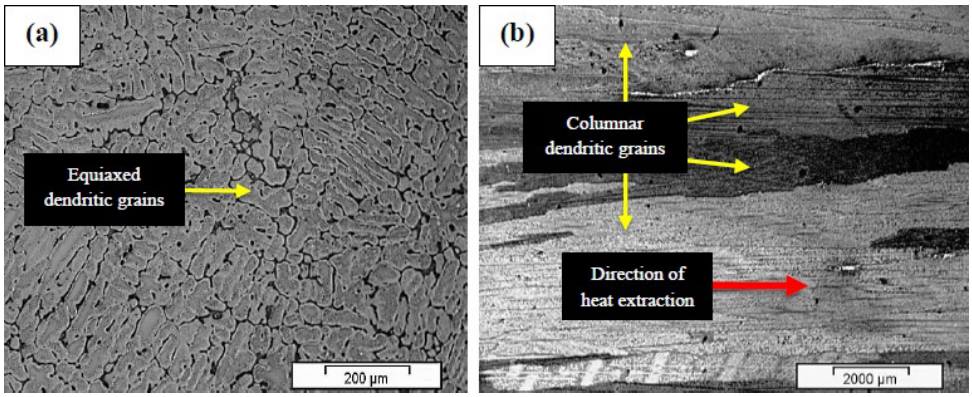

Figure 2. Original macrostructures of the samples solidified (a) Conventionally (b) Unidirectionally.

temperatures of 250, 300, 350, 400 and 450 ºC during 1 hour. The temperatures used were stipulated according to the literature[30]. explains that the ideal recrystallization temperature to be used in aluminum alloys that were previously cold-worked start from 340° up to 400 °C, but these temperatures and the rate of heating are specific for each alloy, and have to be carefully studied[31]. also studied the recrystallization of an aluminium alloy, the 7075. The temperatures of annealing used in their research were of 100 - 400 ºC during 1 hour. The time of 1 hour was arbitred according to[32]. They indicate that the annealing times for aluminium alloys after cold working vary from 20 to 60 minutes, depending on the content of the alloy. It is known that times above 1 hour might result in grain growth. The recrystallization kinetics was evaluated at the times of 1, 5, 10, 15, 20, 30, 40, 50 and 60 minutes. It had the objective to determine the smaller temperature necessary to recrystallize the Al 4,5% Cu alloy, and what condition (conventional and unidirectional) would recrystallize in smaller temperature. The recrystallization kinetics is defined as the variation in the fraction of recrystallized volume. It is dependent to the annealing time at isothermal conditions[33]. The heat treatments were performed in an EDG® 3P-S furnace.

In order to observe the microstructure of the samples, a chemical attack was performed using an etching solution (Keller) with times ranging up to 10 seconds. After attack, the samples were analyzed in a Carl Zeiss® Jenavert optical microscope, at magnifications of 50, 200 and 500 x. Also, a scanning electron microscope Carl Zeiss® EVO MA 15 was used in the backscattered electron detector (BSD) with magnification of 200 x, energy dispersive spectroscopy (EDS) and mapping modes. The microhardness was performed using a Digimess® HV-1000 microdurometer. For each sample, 20 indentations were applied at each treatment temperature, proceeding with the calculation of the mean and standard deviation. The technical standard used was the[34], which indicates the procedure to measure the Vickers hardness in metallic materials. A square-based pyramid indenter was used, with face angles of 136 º and penetration load of 0.198 N. This test indicated the influence of microstructural changes in the Vickers microhardness of the Al4.5wt%Cu alloy solidified through different methods.

3. Results and Discussion

3.1 Original microstructure

Figure 2 shows the optical analysis of the Al4.5wt%Cu alloy, in longitudinal section from the crude solidification process, without any PD. In Figure 2a, it is possible to see the Al4.5wt%Cu alloy with its original microstructure, after conventional solidification. It is remarkable the presence of equiaxed dendritic grains, with equivalent size and dimensions in all directions. In Figure 2b, it is observed after unidirectional solidification, columnar dendritic grains that grew in the direction of the flow of heat extraction.

3.2 Microstructure versus microhardness after RA

Figure 3 shows the longitudinal microstructure of Al4.5wt%Cu alloy after conventional solidification. Figures 3a, 3b and 3c refer to the samples after cold rotary forging, with 54, 76 and 91% of RA, respectively. It can be observed the elongation of the grains along the direction in which the material was conformed. As the RA increases, the grains become flatter. Also, the $CuAl_2$ precipitates get closer to each other, once that they are located at the grain boundaries. Other authors such as[35] found as well $CuAl_2$ precipitates at the grains boundaries of the casted Al4.5wt%Cu alloy. They explain that these precipitates are formed during the cooling process, after solidification. It happens due to the chemical driving force caused by large Cu supersaturation, at or near these grain boundaries. Also, it acts like preferred sites for

In Figure 4, the microstructure of Al-4.5Wt%Cu alloy can also be seen in longitudinal section, after unidirectional

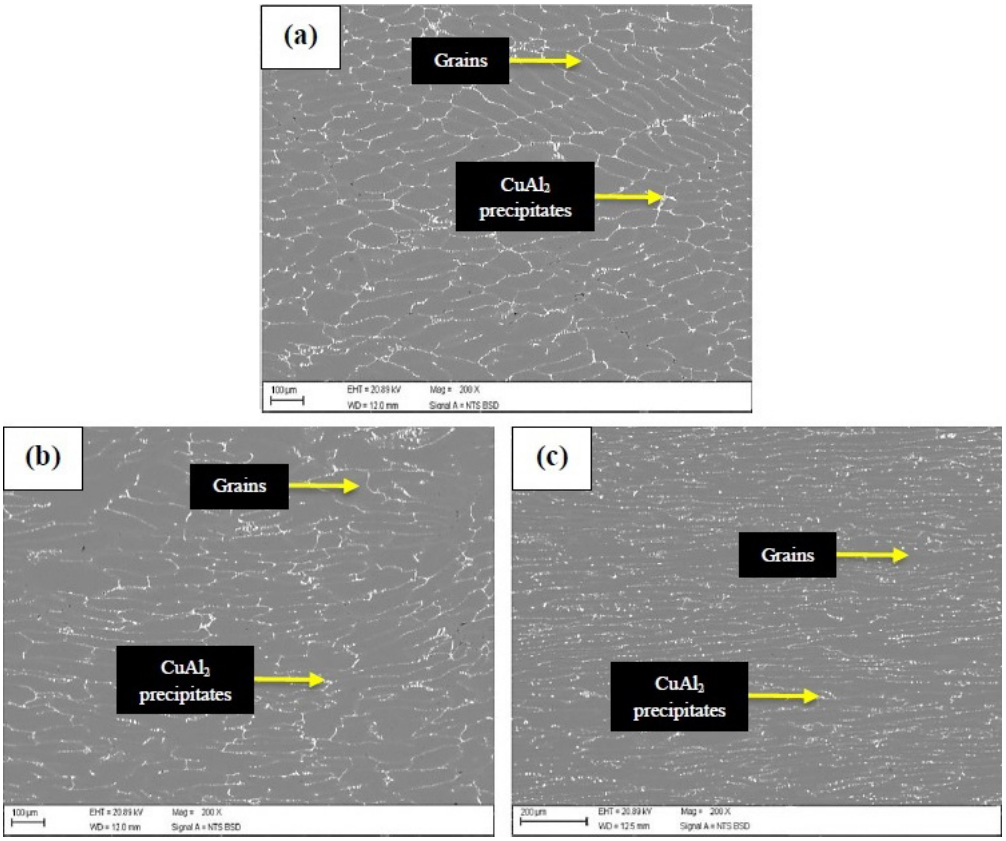

Figure 3. Microstructure of the Al4.5wt%Cu alloy after conventional solidification and RA of (a) 54% (b) 76% (c) 91%.

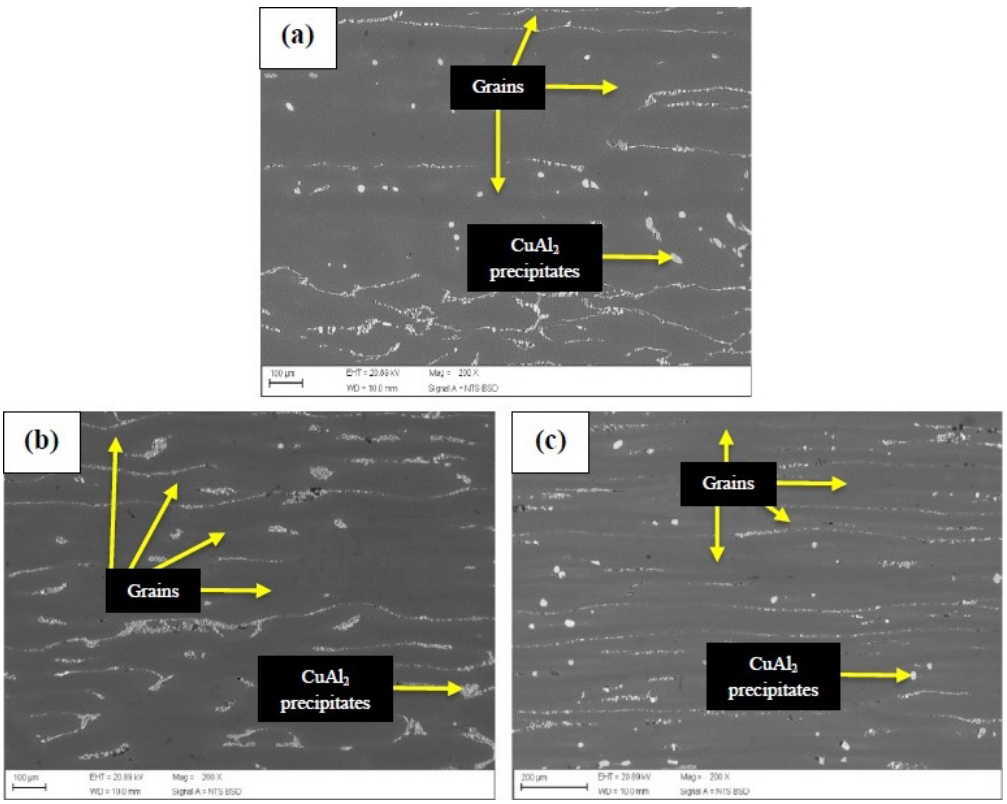

Figure 4. Microstructure of the Al4.5wt%Cu alloy after unidirectional solidification and RA of (a) 54% (b) 76% (c) 91%.

solidification. Figures 4a, 4b and 4c evidence, by the same way that Figure 3 that, the higher is the RA, smaller is the spacing between the grains, that become flatter and more elongated. However, differently from the conventional solidification, for unidirectional solidification, the grains boundaries are more spaced from each other. It is due to the shape of these grains, that present a more elongated morphology and a higher spacing between each other. Also, $CuAl_2$ precipitates can be seen as well within the grains, and not only at their boundaries.

As observed in Figures 3 and 4, the morphology of the $CuAl_2$ precipitates change according to their location. For the conventional solidification, they are located at the grain boundaries and present spherical geometry. Already for the unidirectional solidification, these precipitates when situated at the grain boundaries show elongated morphology, but when positioned within the grain, have spherical morphology.

The graph of Figure 5 shows the microhardness of the Al4.5wt%Cu alloy conventionally and unidirectionally solidified before and after RA. For the conventional crude sample, the value of microhardness was of 53.3 HV. After RA of 54, 76 and 91%, the values increased to 72.7, 72.4 and 77.2 HV. For the unidirectional crude sample, a microhardness value of 58.7 HV was found. After RA of 54, 76 and 91%, the microhardness increased to 84.9, 82 and 93.8 HV, respectively.

For the two solidification processes, the crude samples presented the lowest values of microhardness among all. From them to 54% of RA, it was noted an average increase of 25 – 30% in the microhardness. From 54% to 76% of RA, virtually no significant change (0,4 – 3%) was observed. Lastly, from 76 to 91% of RA, a small increase of 6 –12% was verified. Already from the crude samples to 91% of RA, an increase of 31 – 38% was obtained.

The increase in the microhardness values after RA is explained due to the strain hardening (or cold working). Through forming processes, such as forging, extrusion and rolling, the alloy is deformed in order to obtain the final desirable shape. This forming induces the material to a PD, and it creates a great number of new dislocations in its microstrucuture. The increase in the volume of dislocations is the mechanism that enhances the mechanical strength of metals, because one dislocation gets in the way of another,

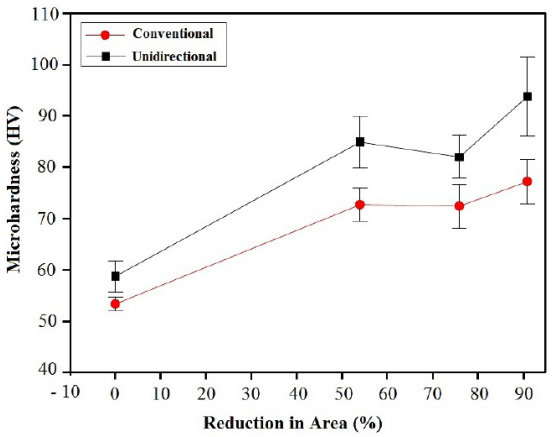

Figure 5. Microhardness of the Al4.5wt%Cu alloy conventionally and unidirectionally solidified before and after 54, 76 and 91% of RA.

providing then obstacles to their motion. Anything that acts as obstacles to the dislocations movement, decreases the ease of PD, and consequently, strengthen the material. It explains the fact that the higher was the RA in Figure 5, the higher were the microhardness values, for both conventional and unidirectional solidification. Another parameter observed in the case of the Al4.5wt%Cu alloy is the presence of $CuAl_2$ precipitates. They behave like a barrier to the dislocations movement within the grains, as well as the grain boundaries do, which enhances the mechanical strength of this alloy through hardening[36,37].

It was also verified that the Al4.5wt%Cu alloy conventionally solidified presented microhardness values subtly lower than those found in the Al4.5wt%Cu alloy unidirectionally solidified. According to the micrographical analysis of Figures 3 and 4, the samples unidirectinally solidified presented $CuAl_2$ precipitates not only at the grain boundaries, as in the Al4.5wt%Cu alloy conventionally solidified, but also within the grains. It provides a higher volume os these precipitates to the Al4.5wt%Cu unidirectinally solidified, and consequently, higher microhardness values.

3.3 Heat treatments

3.3.1 250 to 300 ºC

Figure 6 shows the micrographs of the Al4.5wt%Cu alloy conventionally and unidirectionally solidified after 54, 76 and 91% of RA and heat treatment of 250 and 300 ºC. According to Figure 6, new grains where not formed in the microstructure of the samples treated at 250 and 300 ºC. Microstructurally, only happened the recovery phenomenon. The recovery is the first stage of the isothermal annealing, in which, there is a reaction between punctiform defects leading to a decrease in their quantity and then, annihilation of dislocations of opposite signs and shrinking of dislocations rings. Thus, these dislocations are rearranged to a lower energy configuration, what creates high angle contours. With this, the properties of the material are partially restored to the state before deformation. The speed of recovery decreases over time, as the deformation energy, which is the driving force of the process, is consumed. In polycrystalline materials, the density of dislocations remains high and they continue to accumulate in the grain boundaries. The material still deformed after recovery, which means that the material structure remains under the effects of PD, but presents less internal stresses due to the process of alignment of the dislocations[38,39].

3.3.2 350 ºC

Analyzing the micrographs of the samples solidified conventionally and unidirectionally and heat treated at 350 ºC (Figure 7), it is possible to observe that the conventional sample with 54% of RA presented a greater amount of new grains, when compared to the sample with the same RA but unidirectional solidification. It happened due to the fact that the conventional sample has a greater amount of grain boundaries. As defined by[40], grain boundaries are considered defects related to misorientation of crystal lattices, on the internal interfaces between single crystals, that compose materials with polycrystalline structure. Knowing this[41], explain that where the number of defects is higher when

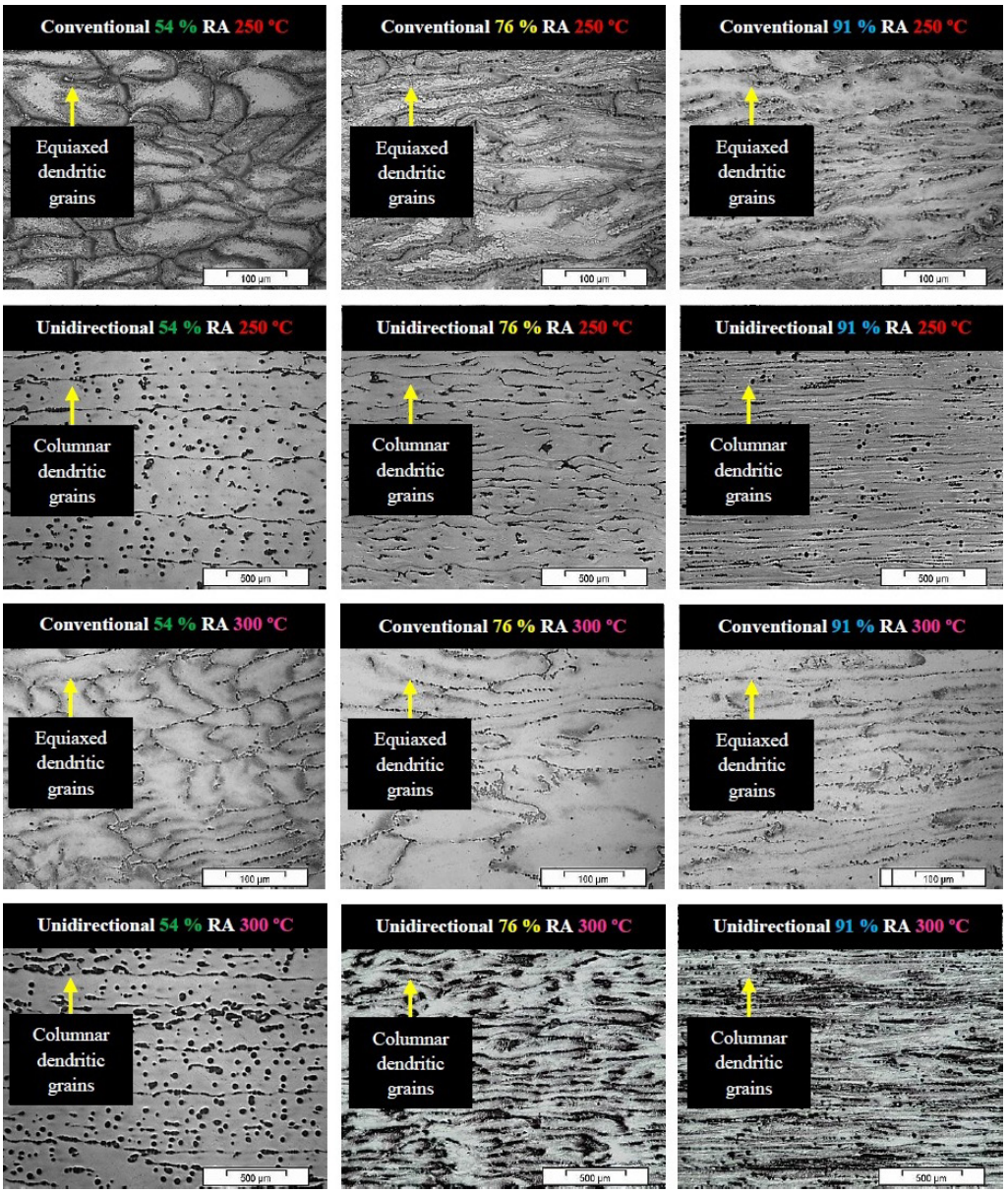

Figure 6. Micrographs of the Al4.5wt%Cu alloy conventionally and unidirectionally solidified after 54, 76 and 91% of RA and heat treatment of 250 and 300 ºC.

compared with other regions of the plastically deformed metal, it is created preferentially sites for the occurrence of recrystallization nucleation. These regions contain "potential nuclei" or "embryos", formed during PD. Another parameter to be considered is the uniformity of the microstucture. According to[42,43], materials subjected to severe PD acquire heterogeneous microstructure. It favors nucleation and recrystallization due to the high energy stored in the microstructure due to strain hardening.

By observing the condition with 76% of RA, the unidirectional sample presented in the $CuAl_2$ precipitates line, the appearance of small grains. Also, in the regions where there is absence of $CuAl_2$ precipitates, the grains have developed with larger dimensions than the grains of the conventional solidified sample. Already for 91% of RA, both conditions presented new grains and $CuAl_2$ precipitates distributted homogeneously along the matrix.

With respect to the recrystallization kinetics, as the recrystallization started at a temperature of 350 ºC for both conditions, the samples with the greatest RA (91%) were treated in times of 1, 5, 10, 15, 20, 30, 40, 50 and 60 minutes, in order to understand the kinetics of recrystallization and its relation to the microhardness values.

Figure 8 shows the micrographs of the recrystallization kinetics for the conventional sample. It was not observed the coexistence of new grains nucleation with recrystallized grains. This is due to the greater amount of energy stored in the microstrucutre of the conventional sample after cold work. The greater amount of grain boundaries causes a high concentration of dislocations and precipitates at these

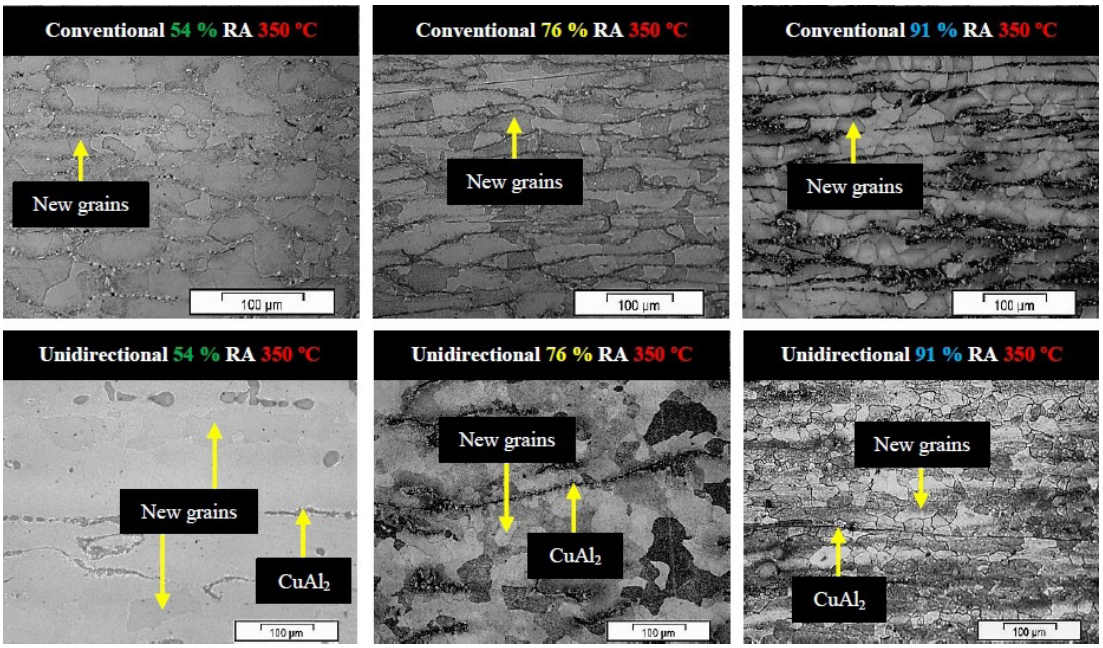

Figure 7. Micrographs of the Al4.5wt%Cu alloy conventionally and unidirectionally solidified after 54, 76 and 91% of RA and heat treatment of 350 ºC.

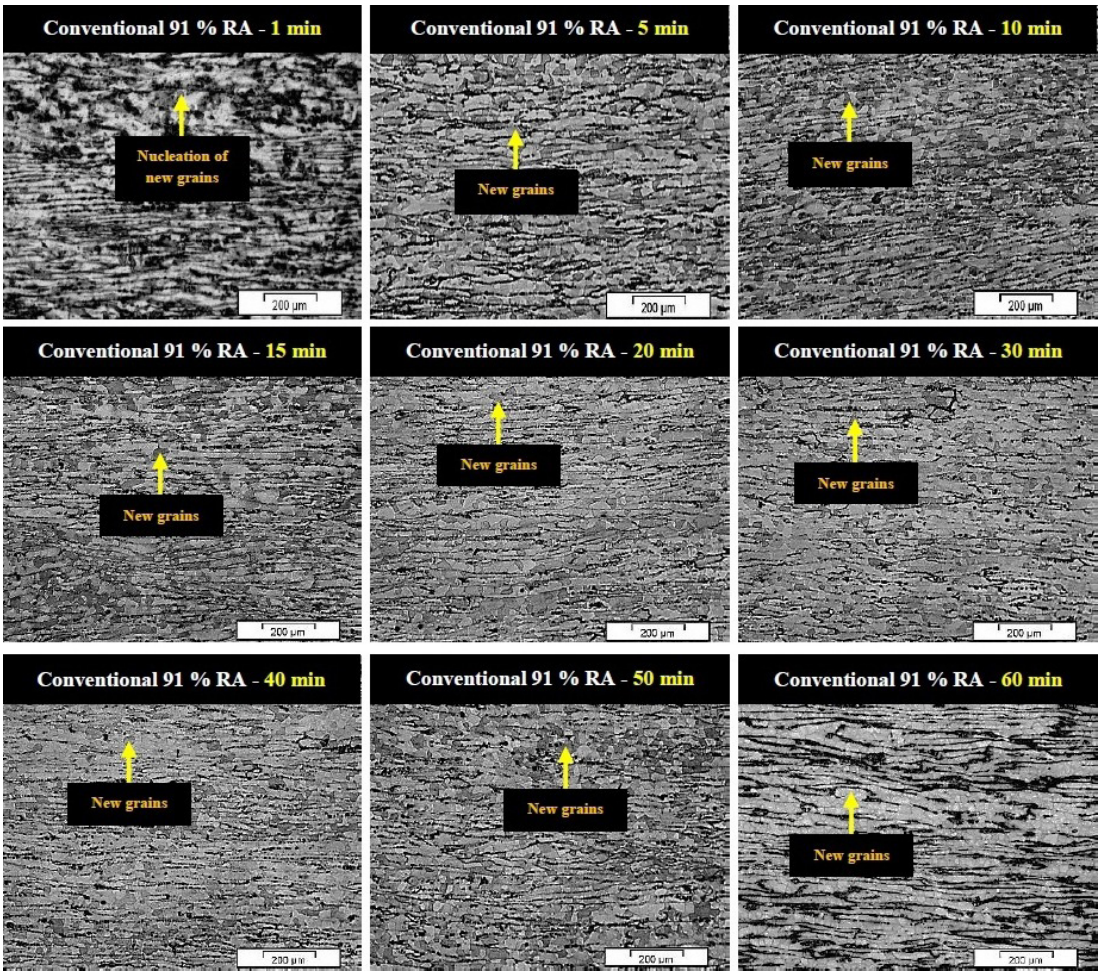

Figure 8. Recrystallization kinetics at 350 ºC of the Al4.5wt%Cu sample with 91% of RA conventionally solidified.

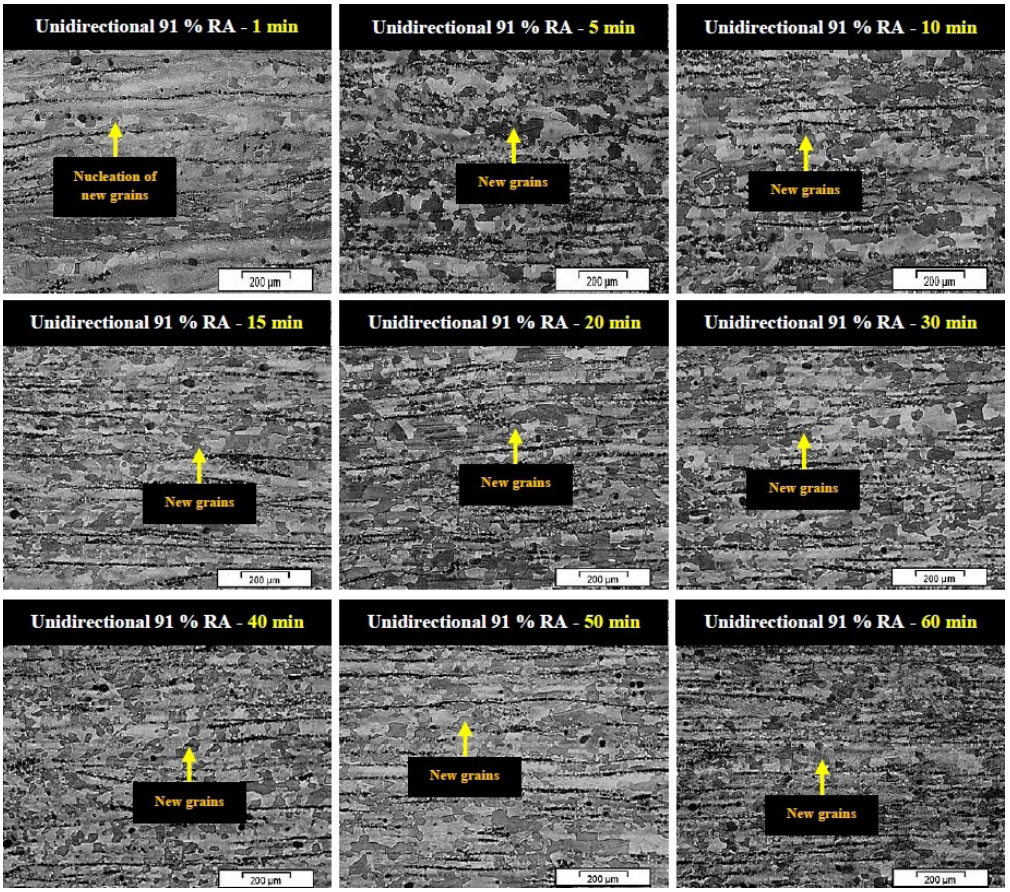

Figure 9. Recrystallization kinetics at 350 ºC of the Al4.5wt%Cu sample with 91% of RA unidirectionally solidified.

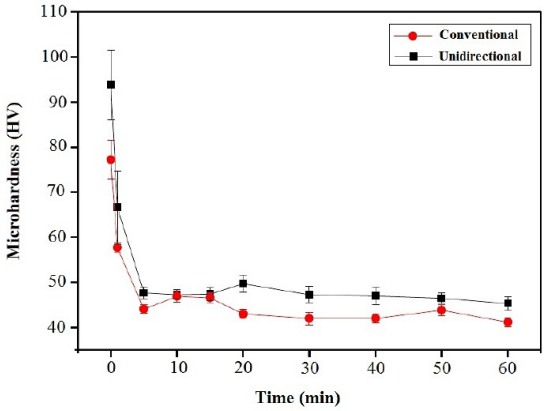

Figure 10. Microhardness after recrystallization kinetics at 350 ºC of the Al4.5wt%Cu sample with 91% of RA conventionally and unidirectionally solidified.

grain boundaries, which provides a more homogeneous distribution of energy, and a greater amount of nuclei to be formed. In the proportion that these grow up, more nuclei are deprived to be formed. In this case, only the migration of high angle contours and grain growth occurs, observed in the photomicrographs of Figure 8 from 5 to 60 minutes.

For the unidirectional sample, after 1 minute of heat treatment (Figure 9), recrystallization can be already observed as partial. This is due to the formation and migration of high-angle contours from pre-existing embryos. It is noted that the emergence of new grains occurs preferably in regions close to the grain boundaries. After 5 minutes, the unidirectional sample shows a large amount of new grains nucleation, as well as grains already recrystallized. The nucleation of new grains decreases with the heat treatment time (10, 15, 20, 30, 40, 50 and 60 minutes). The recrystallized grains use the available thermal energy to increase their dimensions. This can be seen through the photomicrographs of the samples from 5 to 60 minutes.

Figure 10 indicates the microhardness values for the samples with 91% of RA conventionally and unidirectionally solidified. It can be seen that for both conditions, the time of 0 minutes of heat treatment presented the higher values of microhardness, because the samples were still in their original non-recrystallized state. With 5 minutes, after the recrystallization began, the microhardness decreases dramatically. From 10 to 15 minuts, the microhardness of both conditions remained practically the same, with the unidirectional sample presenting a slightly higher value than the conventional sample. Finally, from 15 to 60 minutes, the microhardness values continued practically the same for both conditions, but with the unidirectional samples presenting greater values than the conventional sample. It is explained due to the presence of $CuAl_2$ precipitates within the grains of the unidirectional samples, that act as a reinforcement to the matrix.

3.3.3 400 ºC

According to Figure 11, for the conventional samples with 54, 76 and 91% of RA, the evolution in the grain size is decrescent with the increase of the RA. Also, there is no expressive amount of small grains close to the precipitates. This is due to the fact that the precipitates are delimiting the grain boundaries. After cold work, the grains elongated in the direction of conformation together with the precipitates in their contours, so the amount of energy stored for the nucleation of new grains is practically the same in all regions. Also, no marked difference in grain size after the heat treatment exists, differently from the unidirectional sample.

For the unidirectional samples treated at 400 ºC, it is noted that the grain size for 54% of RA is comparatively much higher than the grain size of the samples submitted to 76 and 91% of RA. This variation in the grain size is justified by the RA imposed on the material.

Authors such as[41,44,45] explain that the greater is the deformation of the material, greater will be the nucleation of new grains. The cold working of metallic materials increases the stored energy on its microstructure, most significantly through an increased dislocation density in the crystal structures. This stored energy due to deformation in the form of crystalline defects is the driving force for recrystallization. It is possible to notice the formation of small nuclei close to the $CuAl_2$ precipitates in all the unidirectional samples to different RA. As previously mentioned, grain and precipitate contours are sources of nucleation of new grains due to the anchoring of dislocations. In grain contour regions where $CuAl_2$ did not precipitate, the nuclei that appeared did not encounter resistance and the growth of high-angle grains occured. However, the nuclei that were formed between the $CuAl_2$ precipitates had limited growth due to the barrier created by the precipitates.

3.3.4 450 ºC

Through the analysis of the photomicrographs of Figure 12, it can be seen that to the conventional samples with 54 and 91% of RA, the second phase of $CuAl_2$ is precipitated within the grains, while in Figure 12 to the conventional sample with 76% of RA, the precipitates are located at the grain boundaries. To the unidirectional samples, the microstructure for the three RA after heat treatment at 450 ºC is completely replaced by new grains. The nucleation still occurs at the grain boundaries, but in a smaller fraction. Comparing Figure 12 to the unidirectional sample with 91% of RA, with Figure 11 over the same condition, it is noted an increase in the grain size from 400 to 450 ºC.

As explained by[46], the grain growth happens when a sorce of heat is applied in the material during a period of time. However, the extent of this grain growth depends of the microstructure nature. In pure metals and solid-solution alloys, the grains grow rapidly at elevated temperatures due to the absence of precipitates within the crystalline lattice, which restricts the movement of the grain boundaries. In the other hand, submicrometer grains may be retained to relatively high temperatures in materials containing a distribution of fine precipitates, such as Al–3%Mg–0.2%Sc alloy containing Al_3Sc precipitates and Al-7034 Al–Zn– Mg alloy containing $MgZn_2$ and Al_3Zr precipitates.

3.3.5 Recrystallization curves

Figure 13 shows the microhardness of the Al4.5wt%Cu alloy solidified conventionally (Figure 13a) and unidirectionally (Figure 13b) after 54, 76 and 91% of RA. As observed in Figure 7, the recrystallization of the conventional and unidirectional samples began at the temperature of 350 ºC. However, while the conventional sample with 54% of RA presented total recrystallization, the unidirectional sample

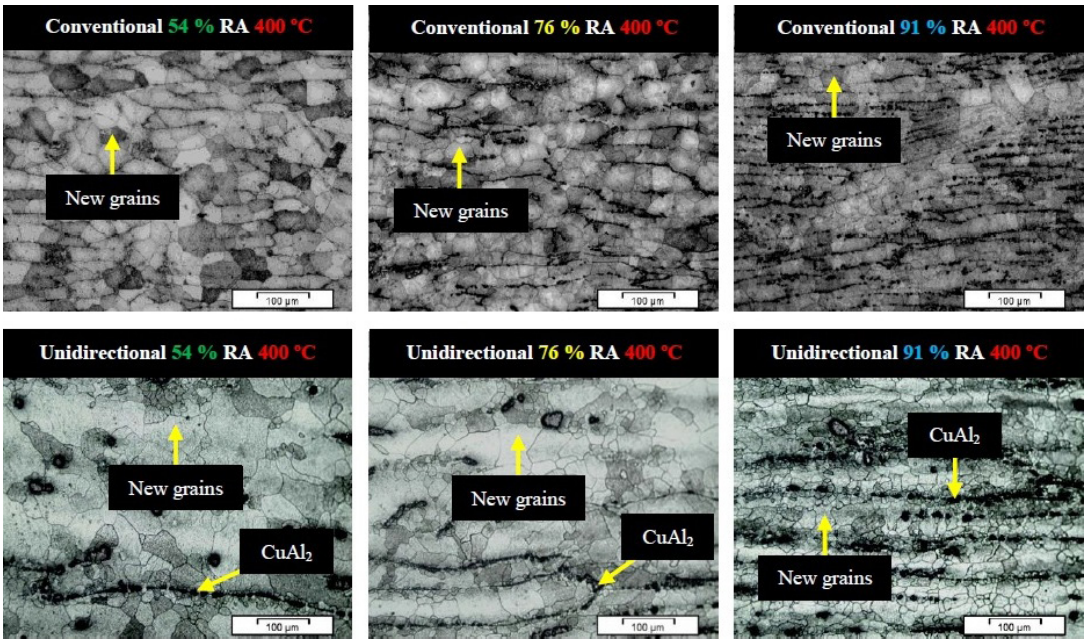

Figure 11. Micrographs of the Al4.5wt%Cu alloy conventionally and unidirectionally solidified after 54, 76 and 91% of RA and heat treatment of 400 ºC.

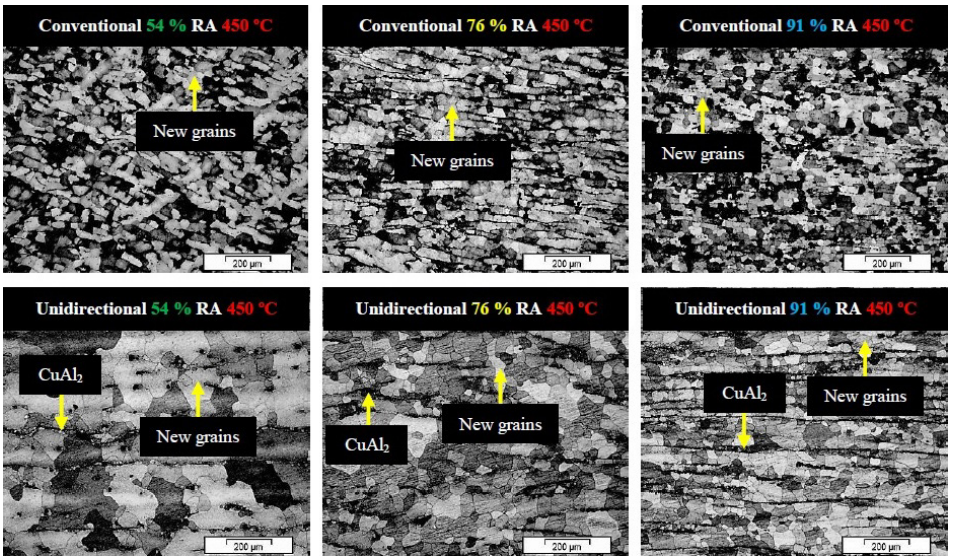

Figure 12. Micrographs of the Al4.5wt%Cu alloy conventionally and unidirectionally solidified after 54, 76 and 91% of RA and heat treatment of 450 ºC.

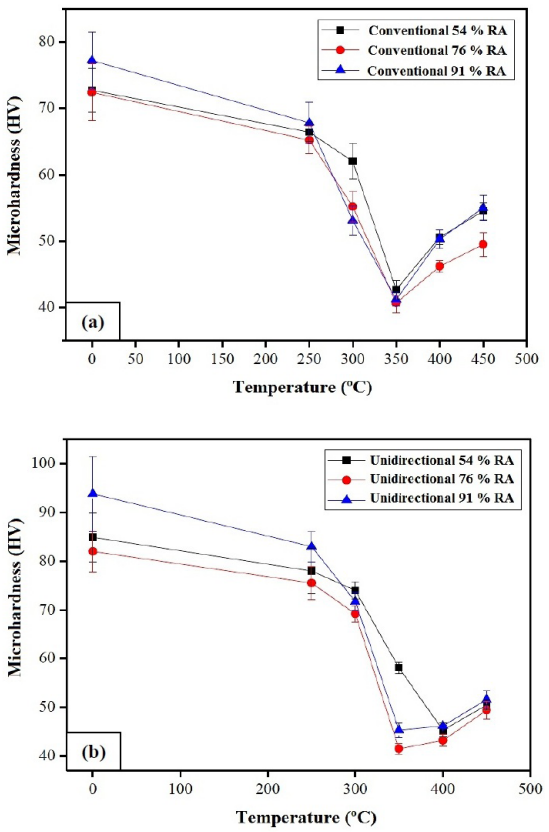

Figure 13. Microhardness of the Al4.5wt%Cu alloy after 54, 76 and 91% of RA solidified (a) Conventionally (b) Unidirectionally.

Table 2. Density of $CuAl_2$ precipitates in the Al4.5wt%Cu alloy.

Solidification	$CuAl_2$ precipitate density (%)			
	Edge		Center	
	350 °C	450 °C	350 °C	450 °C
Conventional	6.27	7.23	6.14	6.85
Unidirectional	6.01	7.97	6.49	7.76

with the same condition obtained only partial recrystallization. This happened because in the conventional sample, there is a homogeneity in the size of the grains, which are delimited by precipitates in their contours. Thus, in the sample with 54% of RA there was enough energy to occur the recrystallization.

From 350 ºC the microhardness starts to rise again for the three RA. However, observing the condition of 76% of RA, a value below of 54 and 91% of RA was obtained. This is due to the presence of $CuAl_2$ precipitates within the grains of the samples with 54 and 91% of RA, as observed in Figure 12, while in the sample with 76% of RA, the presence of these precipitates within the grains was not noticed. This makes the microhardness values to be smaller.

Analyzing the Figure 13b, for the unidirectional samples, it can be observed at temperatures of 250 and 300 ºC that all of the samples decreased the microhardness value regardless of the percentage of RA. However, the temperatures of heat treatment were not sufficient to start the recrystallization. Since this decrease in the microhardness values is small, and in the micrographs of Figure 6 at 300 ºC there was no presence of new grains, it can be can concluded that at this temperature range, only the phenomenon of recovery occurred. At 350 ºC, the sample with 54% of RA presented partial recrystallization. However, the samples conformed at 76 and 91% of RA, there was recrystallization, being capable to obtain microhardness values of 42 and 46 HV, respectively.

3.3.6 $CuAl_2$ precipitate density

Table 2 shows the density of precipitates at temperatures of 350 and 450 ºC. For a better understanding concerning to the increase of the microhardness values at the recrystallization temperatures of 350 to 450 ºC, image analysis was used to assess the density of $CuAl_2$ precipitates. It was taken as a reference the center and the edge of each sample (Figure 14). According to Table 2, with the increase of the temperature, the density of precipitates also increases. This implies in

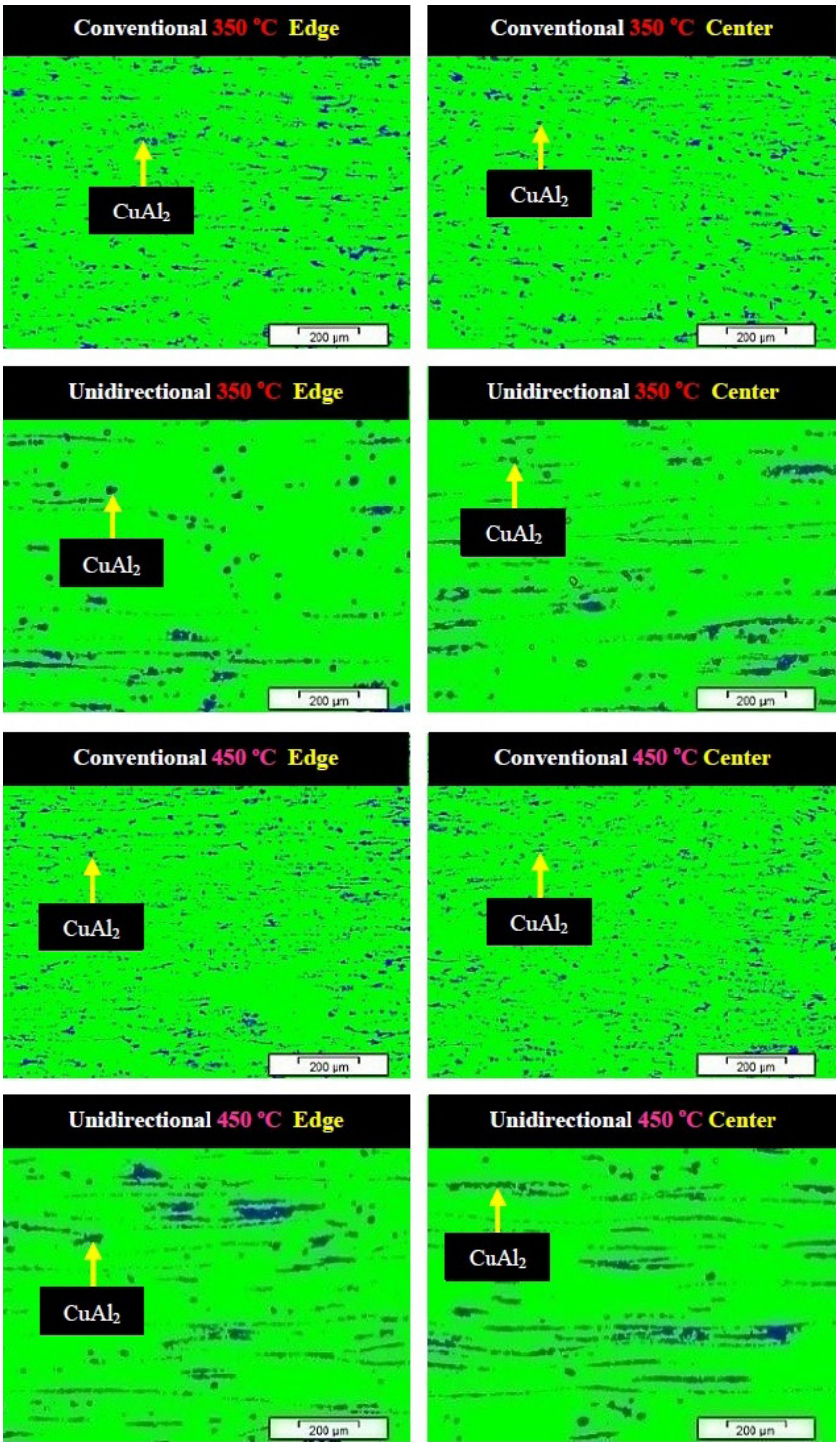

Figure 14. Density of precipitates at 350 and 450 ºC for the Al4.5wt%Cu alloy conventionally and unidirectionally solidified.

a direct increment in the microhardness values, with the increase of the temperature of recrystallization.

Analyzing Figure 14, it is possible to note that the density of precipitates for the conventional sample at 450 ºC was higher at both edge and center, when compared to the samples treated at 350 ºC. The same behavior was observed for the unidirectional samples. This reinforces that the increase in the microhardness values of the conventional and unidirectional samples at temperatures above 350 ºC is due to the formation of a greater amount of $CuAl_2$ precipitates. Also, according to the micrographs, the precipitates in the conventional samples are better distributed and refined than the unidirectional samples, that are presented more grouped and close to each other.

3.3.7 Grain size analysis

To evaluate the grain size of the samples recrystallized at 450 ºC, optical microscopy test was performed in the conventional and unidirectional samples with 54, 76 and 91% of RA. Figure 15 shows the results obtained. It can be seen that the conventional samples presented a small variability in the grain size with the various RA. However, in the unidirectional samples, there is greater variability in the grain size, due to the solidification process. In general, there is a decrease in the grain size values as the RA increases, for both conventional and unidirectional samples. It occurs due to the greater RA imposed in the cold working process, that creates a greater number of nuclei, which limits the grain growth.

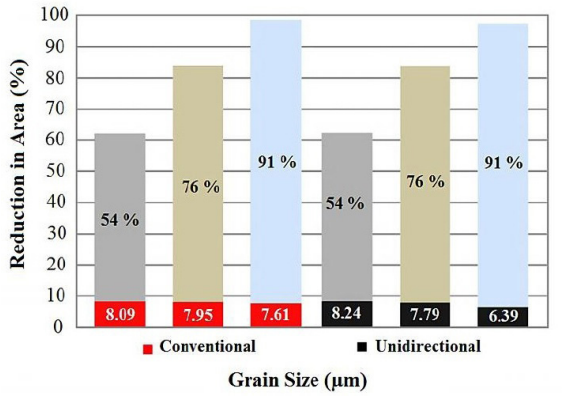

Figure 15. Grain size of the Al4.5wt%Cu alloy conventionally and unidirectionally solidified with 91% of RA and heat treatment of 450 ºC.

Table 3. Quantity by weight of aluminum and copper in the Al4.5wt%Cu alloy.

Solidification	Matrix (% wt)		Precipitate (% wt)	
	Al	Cu	Al	Cu
Conventional	96.1	3.9	64.5	36.5
Unidirectional	97.3	2.7	56.6	43.4

3.3.8 Semi quantitative analysis of aluminum and copper in the matrix and precipitate

To evaluate the quantity by weight of the aluminum and copper elements, semi-quantitative x-ray analysis were used in the scanning electron microscope. The analysis were performed in the matrix and precipitate of both conventional and unidirectional samples. The values found are shown in Table 3. It can be seen that the matrix and the precipitates present values close to each other, with no significant diferences due to the solidification process.

3.3.9 Mapping of the unidirectional sample with 91% RA heat treated at 450 ºC

To assess the distribution of the chemical elements aluminum and copper in the Al4.5wt%Cu alloy matrix, a sample with 91% of RA unidirectionally solidified at 450 ºC was studied by mapping (Figure 16). Figure 16a shows the region of analysis. As it can be observed in Figure 16b, the copper is concentrated in the precipitates, due to the formation of the $CuAl_2$ phase. Also, it is dispersed in the Al matrix (Figure 16c), as small precipitates or as a solid solution.

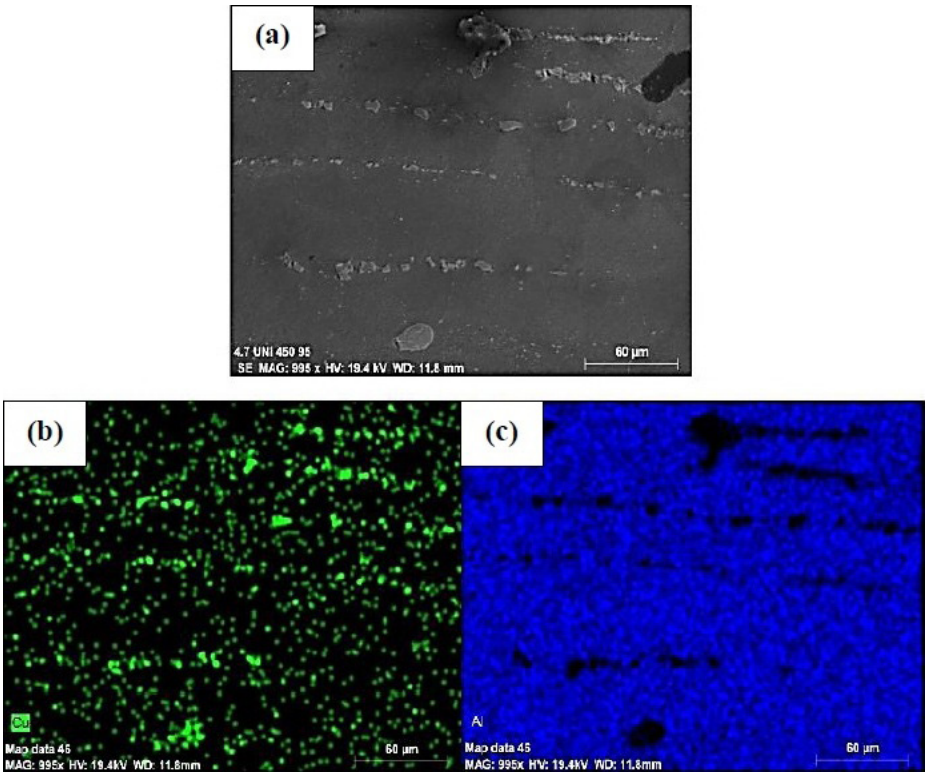

Figure 16. Al4.5wt%Cu alloy unidirectionally solidified with 91% of RA after heat treatment at 450 ºC and mapping analysis.

4. Conclusions

The recrystallization study of the Al4.5wt%Cu alloy conventionally and unidirectionally solidified, deformed and heat treated have been studied. The results indicated that:

- The conventional and unidirectional samples cold-worked with 54, 76 and 91% of RA, recrystallized at temperature of 350 ºC. However, the unidirectional sample with 54% of RA obtained only partial recrystallization.
- In the study of the recrystallization kinetics, the conventional and unidirectional samples presented full recrystallization after 5 minutes of heat treatment at 350 ºC.
- For both conditions, there was an increase in the microhardness values after heat treatment from 350 ºC to 450 ºC.
- The samples solidified conventionally and unidirectionally had close microhardness values after heat treatment of 450 ºC.
- There was a great variability in the final grain size for the unidirectionally solidified samples, which was not observed in the conventionally solidified samples.
- The $CuAl_2$ precipitates were found well dispersed in the Al matrix for both solidification processes.

5. Acknowledgments

The authors would like to thank the CAPES and CNPq for the financial support to develop this work.

6. References

1. Devaraj S, Narayanaswamy KS, Hemanth K, Shamanth V. Processing, microstructure and mechanical behavior of spray casted Al-4.5 wt% Cu alloy. Materials Today: Proceedings. 2020;20:120-4.
2. Zhang J, Song B, Wei Q, Bourell D, Shi Y. A review of selective laser melting of aluminum alloys: Processing, microstructure, property and developing trends. J Mater Sci Technol. 2019;35:270-84.
3. Williams J, Starke EA Jr. Progress in structural materials for aerospace systems. Acta Mater. 2003;51:5775-99.
4. Xu W, Luo Y, Zhang W, Fu M. Comparative study on local and global mechanical properties of bobbin tool and conventional friction stir welded 7085-T7452 aluminum thick plate. J Mater Sci Technol. 2018;34:173-84.
5. Shanmughasundaram P, Dahle AK. Heat treatment of aluminum alloys. In: Hashmi MSJ. Reference module in materials science and materials engineering. Oxford: Elsevier; 2018. p. 1-8.
6. Ma PP, Liu CH, Wu CL, Liu LM, Chen JH. Mechanical properties enhanced by deformation-modified precipitation of θ′-phase approximants in an Al-Cu alloy. Mater Sci Eng A. 2016;676:138-45.
7. Osório WR, Garcia LR, Peixoto LC, Garcia A. A influência da macrosegregação e da variação dos espaçamentos dendríticos na resistência à corrosão da liga Al-4,5%Cu. Revista Matéria. 2008;13:542-52.
8. Taha MA, Elkomy GM, Mostafa HA, Gouda ES. Effect of ZrO_2 contents and ageing times on mechanical and electrical properties of Al–4.5 wt.% Cu nanocomposites prepared by mechanical alloying. Mater Chem Phys. 2018;206:116-23.
9. Schöbel M, Fernández R, Koos R, Bernardi J. Elasto-plastic deformation in Al-Cu cast alloys for engine componentes. J Alloys Compd. 2019;775:617-27.
10. Gao L, Li K, Ni S, Du Y, Song M. The growth mechanisms of θ′ precipitate phase in an Al-Cu alloy during aging treatment. J Mater Sci Technol. 2021;61:25-32.
11. Chen ZW, Gao JP. Formation of twinned dendrites during unidirectional solidification of Al−32%Zn alloy. Trans Nonferrous Met Soc China. 2018;28:802-11.
12. Sakane S, Takaki T, Ohno M, Shibuta Y, Shimokawabe T, Aoki T. Three-dimensional morphologies of inclined equiaxed dendrites growing under forced convection by phase-field-lattice Boltzmann method. J Cryst Growth. 2018;483:147-55.
13. Amoorezaei M, Gurevich S, Provatas N. Orientation selection in solidification patterning. Acta Mater. 2012;60:657-63.
14. Chen Z, Wang E, Hao X. Microstructure and orientation evolution in unidirectional solidified Al–Zn alloys. Mater Sci Eng A. 2016;667:1-8.
15. Sakane S, Takaki T, Ohno M, Shibuta Y. Simulation method based on phase-field lattice Boltzmann model for longdistance sedimentation of single equiaxed dendrite. Comput Mater Sci. 2019;164:39-45.
16. Karagadde S, Bhattacharya A, Tomar G, Dutta P. A coupled VOF–IBM–enthalpy approach for modeling motion and growth of equiaxed dendrites in a solidifying melt. J Comput Phys. 2012;231:3987-4000.
17. Pines V, Chait A, Zlatkowski M, Beckermann C. Equiaxed dendritic solidification in supercooled melts. J Cryst Growth. 1999;197:355-63.
18. Rappaz M, Gandin CA, Desbiolles JL, Thévoz P. Prediction of grain structures in various solidification processes. Metall Mater Trans, A Phys Metall Mater Sci. 1996;27:695-705.
19. Lin X, Huang W, Feng J, Li T, Zhou Y. History-dependent selection of primary cellular/dendritic spacing during unidirectional solidification in aluminum alloys. Acta Mater. 1999;47:3271-80.
20. Baker I. Recovery, recrystallization and grain growth in ordered alloys. Intermetallics. 2000;8:1183-96.
21. Doherty RD, Hughes DA, Humphreys FJ, Jonas JJ, Jensen DJ, Kassner ME, et al. Current issues in recrystallization: a review. Mater Sci Eng A. 1997;238:219-74.
22. Alaneme KK, Okotete EA. Recrystallization mechanisms and microstructure development in emerging metallic materials: a review. Journal of Science: Advanced Materials and Devices. 2019;4:19-33.
23. Baltzer N, Copponnex T. Precious metals for biomedical applications. Cambridge: Woodhead Publishing; 2014. Properties and processing of precious metal alloys for biomedical applications; Vol. 1, p. 1-236.
24. Sarkar J. Sputtering materials for VLSI and thin film devices. USA: Elsevier; 2014. Sputtering target manufacturing; Vol. 1, p. 197-289.
25. Su CW, Lu L, Lai MO. Recrystallization and grain growth of deformed magnesium alloy. Philos Mag. 2008;88:181-200.
26. Sakai T, Belyakov A, Kaibyshev R, Miura H, Jonas JJ. Dynamic and post-dynamic recrystallization under hot, cold and severe plastic deformation conditions. Prog Mater Sci. 2014;60:130-207.
27. Burke JE, Turnbull D. Recrystallization and grain growth. Prog Met Phys. 1952;3:220-44.
28. Louhenkilpi S. Treatise on process metallurgy. Industrial Processes. 2014;3:373-434.
29. Hoffmanner LA. Rotary swaging of bars and tubes: ASM Handbood. Materials Park: ASTM International; 1990. p. 128-44.
30. Singh R. Applied welding engineering: processes, codes, and standards. 2nd ed. USA: Elsevier; 2016. p. 111-24.

31. Souza SH, Padilha AF, Kliauga AM. Softening behavior during annealing of overaged and cold-rolled aluminum alloy 7075. Mater Res. 2019;22:1-9.
32. Rashed HMMA, Bazlur Rashid AKM. Heat Treatment of Aluminum Alloys. In: Hashmi MSJ. Comprehensive Materials Finishing. Oxford: Elsevier; 2017. p. 337-71.
33. Malta PO, Alves DS, Ferreira AOV, Moutinho ID, Dias CAP, Santos DB. Static recrystallization kinetics and crystallographic texture of nb-stabilized ferritic stainless steel based on orientation imaging microscopy. Metall Mater Trans, A Phys Metall Mater Sci. 2017;48:1288-309.
34. ASTM International. ASTM E92-16 - Standard test methods for Vickers hardness and Knoop hardness of metallic materials. West Conshohocken, PA: ASTM International; 2016.
35. Herbert MA, Sarkar C, Mitra R, Chakraborty M. Microstructural evolution, hardness, and alligatoring in the mushy state rolled cast Al-4.5Cu alloy and in-situ Al4.5Cu-5TiB2 composite. Metall Mater Trans, A Phys Metall Mater Sci. 2007;38:2110-26.
36. Mouritz AP. Introduction to aerospace materials. Cambridge: Woodhead Publishing; 2012. p. 1-640.
37. Yin Y, Faulkner R, Starr F. Austenitic steels and alloys for power plants. In: Shirzadi A, Jackson S, editors. Structural alloys for power plants operational challenges and high-temperature materials. Cambridge: Woodhead Publishing; 2014. p. 105-152.
38. Padilha AF, Siciliano F Jr. Encruamento, recristalização, crescimento de grão e textura. 3. ed. São Paulo: Associação Brasileira de Metalurgia, Materiais e Mineração; 2005. p. 1-232.
39. Miller VM, Johnson AE, Torbet CJ, Pollock TM. Recrystallization and the development of abnormally large grains after small strain deformation in a polycrystalline nickel-based superalloy. Metall Mater Trans, A Phys Metall Mater Sci. 2016;47:1566-74.
40. Cleja-Ţigoiu S, Paşcan R, Ţigoiu V. Disclination based model of grain boundary in crystalline materials with microstructural defects. Int J Plast. 2018;114:227-51.
41. Rios PR, Siciliano F Jr, Sandim HRZ, Plaut RL, Padilha AF. Nucleation and growth during recrystallization. Mater Res. 2005;8:225-38.
42. Chen CL, Dong YM, Fu SM. Strain heterogeneity, recovery and recrystallization of nanostructured ods alloys during cold deformation. Mater Trans. 2012;53:1795-800.
43. Ma E, Zhu T. Towards strength–ductility synergy through the design of heterogeneous nanostructures in metals. Mater Today. 2017;20:1-9.
44. Doherty RD, Cahn RW. Nucleation of new grains in recrystallization of coldworked metals. J Less Common Met. 1972;28:279-96.
45. Hallberg H, Adamski F, Baïz S, Castelnau O. Microstructure and property modifications of cold rolled IF steel by local laser annealing. Metall Mater Trans, A Phys Metall Mater Sci. 2017;48:4786-802.
46. Valiev RZ, Langdon TG. Principles of equal-channel angular pressing as a processing tool for grain refinement. Prog Mater Sci. 2006;51(7):881-981.